# Multiple Plasmon Effects in the Energy-Loss Spectra of Electrons in Thin Films

M. Šunjić* and A. A. Lucas†
*International Centre for Theoretical Physics, Miramare, Trieste, Italy*
(Received 23 July 1970)

The interaction of a fast electron (energy $\gtrsim$ 1 keV) with collective modes in a thin metallic or doped semiconductor film is studied, taking explicitly into account bulk and surface effects. Reducing the problem to an exactly soluble quantum-mechanical model, we obtain results to all orders of the interaction and investigate the multiple-plasmon contribution to the electron energy losses. The theory is applied to transmission as well as to reflection and a complete description of the loss spectra is obtained. It is shown that the zero-energy plasmon mode does not cause singularities in the low-energy excitation spectrum. The strength of the many-body processes is given by the "fine-structure constant" $e^2/\hbar v_\perp$, where $v_\perp$ is the electron velocity normal to the surface, and in some cases multiple-plasmon emission becomes important, especially so in the specular reflection at grazing-angle incidence. For a thicker slab ($a \sim 500$–$1000$ Å), this results in a series of sharp peaks in the loss spectrum which have maximum strengths corresponding to several excited plasmons. For a thin slab ($a \sim$ few 100 Å), the dominant contribution to the loss spectrum is a broad structure with a high-energy ($\omega > \omega_p$) tail, characteristic for the recombinational effect of many emitted low-energy plasmons.

## I. INTRODUCTION

The interaction of fast electrons (or other charged particles) with collective excitations in solids (plasmons in metals or doped semiconductors, optical phonons in dielectric crystals) and the resulting electron energy-loss spectra have been extensively investigated, both theoretically[1] and experimentally.[2] This work has provided our basic understanding of the elementary excitations in solids and their spectra. We shall not review the vast literature in this field, but only point out that while a full quantum-mechanical treatment has been developed for an infinite solid,[1] the case of a finite solid (e.g., semi-finite medium or thin film) was usually studied[2,3] in the framework of classical electrodynamics. The fast electron, which is treated as a "white" uniform source of electromagnetic radiation frequencies, loses energy through the resonant interaction with bulk and surface polarization eigenmodes of the material. As we show later, this classical theory corresponds to the first-order (Born) approximation for the transition between quantized polarization eigenstates, and therefore can only describe the over-all excitation of a single plasmon or phonon quantum.

Recently, Lucas, Kartheuser, and Badro[4] worked out the quantum-mechanical formulation of the non-retarded interaction between electrons and long-wavelength optical phonons in thin films, and applied it to the single- and double-phonon excitation losses. In this paper we shall take their Hamiltonian and adapt it to the plasmon case.

In Sec. II we describe the fast electron treated as a classical particle, the plasma oscillations in the slab, and the linear electron-plasmon interaction. We obtain the explicit form of the eigenvectors, dispersion relations, and coupling functions for the bulk and surface plasma modes in the slab. In Sec. III we define the electron energy-loss function and express it in a usual way in terms of a correlation function. By noticing the connection of our system with the forced harmonic oscillator we are able to solve the problem exactly and obtain the loss function which includes the electron-plasmon interaction in all orders.

The importance of the exact description instead of the perturbation approach arises from the fact that the surface-plasmon dispersion curve for a finite slab has a branch which goes to zero in the long-wavelength limit. This means that a combined emission of many low-energy plasmons is *a priori* possible for all energies and could drastically alter the shape of the loss spectrum as compared to the one derived classically.

In Sec. IV we apply this theory to the case of the transmitted beam and in Sec. V to the specularly reflected beam, and obtain a description of the complete loss spectrum. The results show that many-plasmon losses dominate the spectrum when the electron velocity $v_\perp$ normal to the slab surface is smaller than or of the order of $e^2/h$. This condition is not satisfied in usual transmission experiments with very fast electrons, but it can be easily realized for the reflection case either in low-energy electron-diffraction (LEED) experiments or with high-energy beam at grazing incidence.[5] The latter experiment provides the most favorable way of observing the multiple-plasmon effects predicted by the present theory.

In this work we neglect plasmon-photon coupling and excitation damping. The retardation effects were shown by Chase and Kliewer[6] not to be significant for the electron-loss spectrum, and the finite

excitation lifetime can be included in the theory[7] by using a complex dielectric function.

## II. FORMULATION OF PROBLEM

We shall use the Hamiltonian formalism to describe the quantum-mechanical system consisting of an electron and the excitations in a slab of metal or doped semiconductor.[8] Our exactly soluble model Hamiltonian is

$$H = E_e + H_0 + H_I \,, \tag{1}$$

where $E_e$ is the fast-electron energy, $H_0$ is the Hamiltonian of the free plasmon modes of the slab, and $H_I$ describes the electron-plasmon coupling.

### A. Electron

We treat the electron (or any other charged particle used in the experiment) as a nonrelativistic particle of velocity $v$ and kinetic energy $E_e = \frac{1}{2}mv^2$ so high that the plasmon field sees it as an infinite reservoir of energy and momentum. This approximation of a recoilless electron is valid, e.g., for $E_e \gtrsim 1$ keV in metallic films with plasmon energies $\hbar\omega_p \lesssim 20$ eV. Thus we consider the electron as a classical particle on the well-defined trajectory $\vec{r}(t)$ acting as a source of time-dependent perturbation for the slab.

### B. Slab

For the slab we assume that it is a plasmon system, i.e., it contains only one type of excitations. In principle, however, it is possible to generalize the theory to include interactions with various fields in the slab (e.g., plasmons plus phonons).

The plasmon modes are described in the continuum approximation, i.e., we consider only long-wavelength excitations, neglecting the spatial dispersion of volume plasmons. In order to write explicitly the Hamiltonian $H_0$ of the free plasmons and the interaction energy $H_I$, we need the eigenvalues and eigenvectors of the polarization modes of the slab. These have already been described in the microscopic theory[4,9] for the optical-phonon case and we here briefly review the results which we shall need later.

Let $\omega_T$ and $\omega_L$ be the transverse and longitudinal optical-phonon frequencies of a polar crystal with a dielectric constant

$$\epsilon(\omega) = \epsilon_\infty(\omega_L^2 - \omega^2)/(\omega_T^2 - \omega^2) \,, \tag{2}$$

where the high-frequency dielectric constant $\epsilon_\infty$ will be taken equal to 1 (point-ion model). Equation (2) satisfies the Lyddane-Sachs-Teller relation[10]

$$\epsilon_0 = \epsilon_\infty \omega_L^2/\omega_T^2 \,, \tag{3}$$

where $\epsilon_0$ is the static dielectric constant.

The nonretarded Maxwell's equations applied to a crystal slab lead to a set of long-wavelength phonon eigenmodes of $P$ polarization.[11] These eigenmodes are characterized by the index $i \equiv (\vec{k}, m, p)$, where $\vec{k}$ is a two-dimensional wave vector parallel to the slab, $m$ is a non-negative integer such that $m/2L$ (where $L = 2a$ is the slab thickness) plays the role of a "quantized" wave vector perpendicular to the slab, and $p = \pm 1$ is the parity of the mode. All the modes with $m \neq 0$ are degenerate at either the longitudinal or the transverse frequency and have sinusoidal polarization patterns typical for the bulk mode (see eigenvectors in Table I). The modes $(\vec{k}, 0, \pm 1)$ are the two surface modes with dispersion relation[4,9]

$$\omega_\pm(\vec{k}) = \omega_T\left[1 + (\omega_p^2/2\omega_T^2)\,(1 \pm e^{-2ka})\right]^{1/2} \,, \tag{4}$$

where

$$\omega_p = \omega_T(\epsilon_0 - 1)^{1/2} \tag{5}$$

is the ion plasma frequency. The corresponding polarization patterns (see Table I) are peaked at the surfaces and decay exponentially on both sides of each surface.

The eigenvectors $\vec{\pi}_{mp}(\vec{k}, z)$ of all the eigenmodes satisfy the orthonormality and closure relations[4]

$$\int_{-a}^{+a} \vec{\pi}^*_{mp}(\vec{k}, z) \cdot \vec{\pi}_{m'p'}(\vec{k}, z)\, dz = \delta_{mm'}\,\delta_{pp'} \,, \tag{6}$$

$$\sum_{mp} \vec{\pi}^*_{mp}(\vec{k}, z)\, \vec{\pi}_{mp}(\vec{k}, z') = \vec{\vec{E}}\,\delta(z - z') \,, \tag{7}$$

where $\vec{\vec{E}}$ is the $(2\times 2)$ unit tensor.

We shall use these results to obtain the microscopic description of the plasma oscillations in a slab. The connection between the optical phonons and the plasmons is obtained by using the limiting prescription[12]

$$\omega_T \to 0, \quad \epsilon_0 \to \infty$$
$$\lim_{\omega_T \to 0,\ \epsilon_0 \to \infty} \omega_T \sqrt{\epsilon_0} = \omega_p \,. \tag{8}$$

Then Eq. (3) gives $\omega_L = \omega_p$, the dielectric function (2) goes into

$$\epsilon(\omega) = 1 - \omega_p^2/\omega^2 \tag{9}$$

and the dispersion relation (4) becomes

$$\omega_\pm(\vec{k}) = (\omega_p/\sqrt{2})\,(1 \pm e^{-2ka})^{1/2} \,. \tag{10}$$

The corresponding eigenvectors (Table I) remain unchanged as they depend only on the geometry of the system and not on the eigenfrequencies.

One recognizes in (9) and (10) the usual dispersion laws for a compensated electron gas of plasma frequency $\omega_p$ in a metallic film[13] [see Fig. 1(a)]. The limiting procedure (8) means, on the one hand, that a free-electron gas has a vanishing shear modulus ($\omega_T \to 0$) and, on the other hand, that the longitudinal optical modes of the ion plasma should correspond to the long-wavelength density fluctuations of the electron plasma ($\omega_L = \omega_p$).

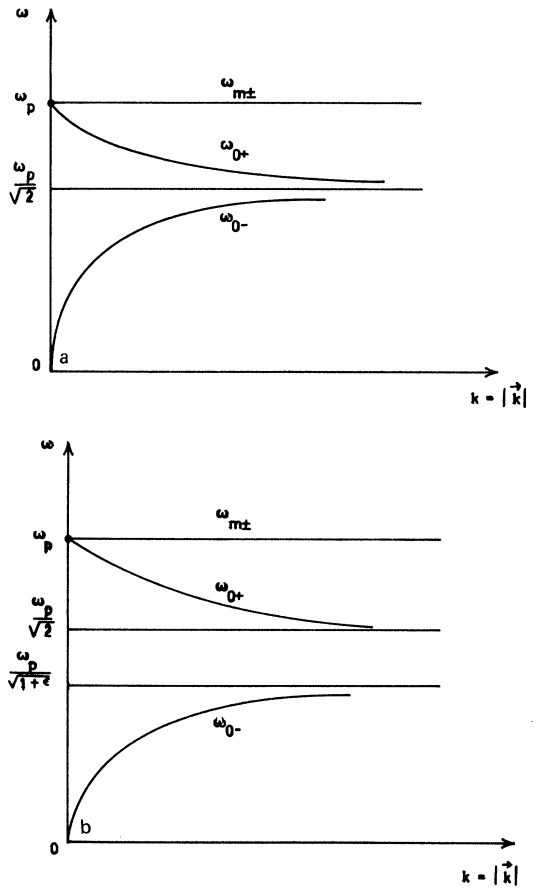


FIG. 1. (a) Plasmon dispersion relation for a metallic slab in vacuum. There are two flat bulk plasmon branches at frequencies $\omega_p$ and zero ("shear" modes). The lower surface plasmon branch $\omega_{0-}$ goes to zero as $\sqrt{k}$. (b) Same for a metallic film deposited on a substrate with a high-frequency dielectric constant $\epsilon$.

The orthonormality and closure relations (6) and (7) allow one to expand the polarization field in terms of annihilation and creation operators $a_i, a_i^\dagger$ for free-plasmon quanta.[4] The free-plasmon Hamiltonian then takes the form

$$H_0 = A \int d\vec{k} \sum_{mp} \hbar\omega_{mp}(\vec{k}) \left[a^\dagger_{mp}(\vec{k}) a_{mp}(\vec{k}) + \tfrac{1}{2}\right], \qquad (11)$$

where the $a_i$ satisfy the quantization relations[4]

$$[a_{mp}(\vec{k}), a^\dagger_{m'p'}(\vec{k}')]_- = (1/A)\,\delta(\vec{k}-\vec{k}')\,\delta_{mm'}\,\delta_{pp'}, \qquad (12)$$

and where $A$ is a unit area of the slab surface.

### C. Electron-Plasmon Interaction

The electron with coordinates $\vec{r}_e = (\vec{\rho}_e, z_e)$ couples to the degenerate bulk plasmons of frequency $\omega_p$ and also to the divergence-free surface plasmons $\omega_\pm(k)$.[4] It does not interact[4] with the zero-frequency "shear" modes of $S$ or $P$ polarization. The interaction Hamiltonian

$$H_I = A \int d\vec{k}\, e^{-i\vec{k}\cdot\vec{\rho}_e} \sum_{mp} \Gamma_{mp}(k, z_e)\left[a^\dagger_{mp}(\vec{k}) + a_{mp}(\vec{k})\right] \qquad (13)$$

is linear in the plasmon field operators.[4] The coupling functions $\Gamma$ are defined by

$$\Gamma_{mp}(k, z_e) = g_{mp}(k) \int_{-a}^{+a} dz\, e^{-k|z-z_e|}\, \vec{\chi}\cdot\vec{\pi}^*_{mp}(k, z), \qquad (14)$$

where

$$g_{mp}(k) = \left[(\hbar e^2 \omega_p^2 / 8\pi A \omega_{mp}(k))\right]^{1/2}, \qquad (15)$$

$$\vec{\chi} = [i, \mathrm{sign}(z_e - z)]. \qquad (16)$$

The explicit form of the coupling functions $\Gamma_i$ is obtained by inserting into (14) the eigenvectors listed in Table I, and the result is given in Table II and illustrated in Fig. 2.

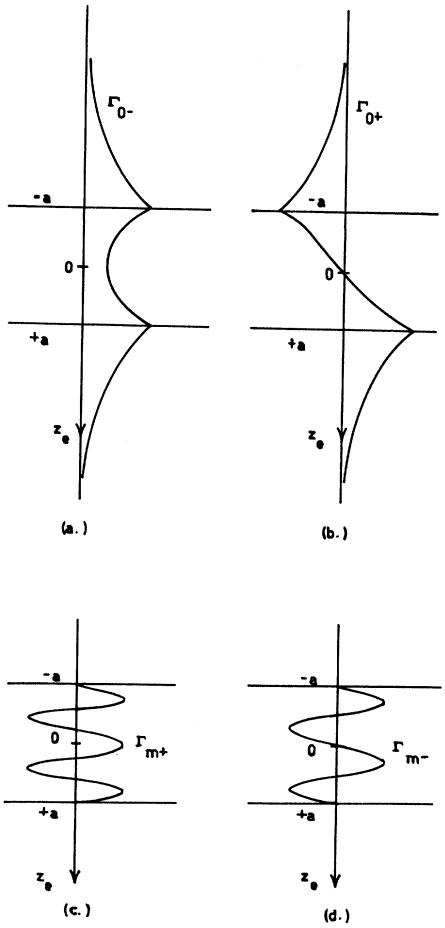


FIG. 2. Spatial dependence of the electron-plasmon coupling functions $\Gamma_i(k, z_e)$. (a) and (b) give the coupling strength for the two surface modes. (c) and (d) correspond to the volume plasmon modes. The "shear" modes are not coupled to the electron.

TABLE I. $P$-polarization plasmon eigenmodes in a slab. The zero-frequency modes have been included for completeness although they do not interact with the electron.

| Eigenvalues | Eigenvectors $\vec{\pi}$ | $m$ |
|---|---|---|
| $\omega_{0-}(k)$ | $\vec{\pi}_{0-} = C_0(i\cosh kz,\ \sinh kz)$ | 0 |
| $\omega_{0+}(k)$ | $\vec{\pi}_{0+} = C_0(i\sinh kz,\ \cosh kz)$ | 0 |
| $\omega_p$ | $\vec{\pi}^L_{m-} = C_m\left[ika\sin\left(\frac{m\pi}{2a}\right)z,\ \frac{1}{2}m\pi\cos\left(\frac{m\pi}{2a}\right)z\right]$ | 2, 4, 6, ... |
| $\omega_p$ | $\vec{\pi}^L_{m+} = C_m\left[ika\cos\left(\frac{m\pi}{2a}\right)z,\ -\frac{1}{2}m\pi\sin\left(\frac{m\pi}{2a}\right)z\right]$ | 1, 3, 5, ... |
| 0 | $\vec{\pi}^T_{m-} = C_m\left[\frac{1}{2}m\pi\cos\left(\frac{m\pi}{2a}\right)z,\ ka\sin\left(\frac{m\pi}{2a}\right)z\right]$ | 2, 4, 6, ... |
| 0 | $\vec{\pi}^T_{m+} = C_m\left[-\frac{1}{2}im\pi\sin\left(\frac{m\pi}{2a}\right)z,\ ka\cos\left(\frac{m\pi}{2a}\right)z\right]$ | 1, 3, 5, ... |

$C_0 = (k/\sinh 2ka)^{1/2}$ ; $C_m = (1/\sqrt{a})\,(k^2a^2 + \frac{1}{4}m^2\pi^2)^{-1/2}$

## III. LOSS SPECTRUM

### A. Evolution of Plasmon State

According to our assumption, the electron is treated as a source of time-dependent perturbation acting on the plasmons in the slab with the trajectory $[\vec{\rho}_e(t), z_e(t)]$. Then the Hamiltonian of the perturbed plasmon field takes the form

$$H_0 + H_I(t) = \sum_i [\hbar\omega_i (a_i^\dagger a_i + \tfrac{1}{2}) + F_i(t)(a_i^\dagger + a_i)], \quad (17)$$

where $i = (\vec{k}, m, p)$ and

$$F_i(t) = e^{-i\vec{k}\cdot\vec{\rho}_e(t)}\,\Gamma_{mp}[k, z_e(t)] .$$

The plasmon state vector in the interaction representation

$$|\psi^I(t)\rangle = e^{(i/\hbar)H_0 t}|\psi^s(t)\rangle \quad (18)$$

satisfies the evolution equation

$$i\hbar\frac{d}{dt}|\psi^I(t)\rangle = V_I(t)|\psi^I(t)\rangle , \quad (19)$$

where

$$V_I(t) = e^{(i/\hbar)H_0 t} H_i e^{-(i/\hbar)H_0 t}$$

$$= \sum_i F_i(t)(a_i^\dagger e^{i\omega_i t} + a_i e^{-i\omega_i t}) . \quad (20)$$

The solution of (19) is given by

$$|\psi^I(t)\rangle = \exp\left(-\frac{i}{\hbar}\sum_i (I_i a_i + I_i^* a_i^\dagger)\right)|\psi^I(t_0)\rangle , \quad (21)$$

where

$$I_i(t, t_0) = \int_{t_0}^{t} dt'\, F_i(t') e^{-i\omega_i t'} . \quad (22)$$

Usually one needs only $I_i(-\infty, +\infty)$, and these functions are listed in Table II for the transmission case and normal incidence ($\vec{\rho}_e = 0$). From (18) and (21) one obtains the state vector of the plasmon field in the Schrödinger representation

$$|\psi^s(t, t_0)\rangle = \exp\left(-\frac{i}{\hbar}H_0 t\right)\exp\left(-\frac{i}{\hbar}\sum_i (I_i a_i + I_i^* a_i^\dagger)\right)$$

$$\times \exp\left(\frac{i}{\hbar}H_0 t_0\right)|\psi^s(t_0)\rangle . \quad (23)$$

### B. Loss Function

The energy spectrum of the outgoing electrons will be described by the loss function $P(\omega)$ giving the intensity of electrons which have suffered a loss of energy $\hbar\omega$ transferred to the excitations of the slab. $P(\omega)$ is therefore defined as the probability that at time $t \to \infty$ the plasmon modes are found in any of the excited states $|[i]\rangle$ of the free Hamiltonian $H_0$ with a total energy $E_{[i]} = E_0 + \hbar\omega$ at $\hbar\omega$ above the initial state energy $E_0$. If we neglect the temperature effects, which are not important in the plasmon energy range, the initial state $|\psi^s(t_0)\rangle$ at $t_0 \to -\infty$ is the ground state $|0\rangle$ of $H_0$. From this definition it follows that:

$$P(\omega) = \lim_{t\to+\infty,\ t_0\to-\infty} \sum_{[i]} |\langle\psi^s(t, t_0)|[i]\rangle|^2$$

$$\times\, \delta\left(\omega - \frac{1}{\hbar}(E_{[i]} - E_0)\right) , \quad (24)$$

where $|\psi^s(t, t_0)\rangle$ is the final state (23) of the slab which, in general, contains all possible multiple excited states

$$|[i]\rangle = |\vec{k}_1^{n_1}, \vec{k}_2^{n_2}, \ldots\rangle = \prod_i \frac{(a_i^\dagger)^{n_i}}{\sqrt{n_i!}}|0\rangle . \quad (25)$$

It is important at this stage to avoid specifying the final state in terms of a few lowest excitations. This would amount to the usual perturbation treatment. Instead, the summation over $[i]$ in (24) can be done by writing the energy-conserving $\delta$ function in the integral form

$$\delta\left(\omega-\frac{1}{\hbar}(E_{[i]}-E_0)\right)$$

$$=\frac{1}{2\pi}\int_{-\infty}^{+\infty}dt\exp\left(\frac{i}{\hbar}(\hbar\omega-E_{[i]}+E_0)t\right)\ . \qquad (26)$$

Inserting (23) into (24) and taking the indicated time limits, the resulting loss function is found to be

$$P(\omega)=\frac{1}{2\pi}\int_{-\infty}^{+\infty}e^{i\omega t}P(t)\,dt\ , \qquad (27)$$

with the correlation function $P(t)$ given by

$$P(t)=\langle 0\,|U^\dagger(t)\,U(0)\,|0\rangle\ , \qquad (28)$$

where

$$U=\exp\left(-\frac{i}{\hbar}\sum_i\,(I_i a_i+I_i^* a_i^\dagger)\right)\ , \qquad (29)$$

$$U(t)=e^{iH_0t}Ue^{-iH_0t} \qquad (30)$$

$$U(t)=\exp\left(-\frac{i}{\hbar}\sum_i\,(I_i a_i e^{-i\omega_i t}+I_i^* a_i^\dagger e^{i\omega_i t})\right)\ . \qquad (31)$$

To calculate $U^\dagger(t)\,U(0)$ we use the Baker-Hausdorf formula $e^Ae^B=e^{A+B+(1/2)[A,B]}$, which holds when $[A,B]$ is a $c$ number. Thus we get all boson operators in the exponent

$$P(t)=\exp\left(-i\sum_i\frac{|I_i|^2}{\hbar^2}\sin\omega_i t\right)$$

$$\times\left\langle 0\left|\exp\left(\frac{i}{\hbar}\sum_i\,[I_i(e^{-i\omega_i t}-1)a_i\right.\right.\right.$$

$$\left.\left.\left.+I_i^*(e^{i\omega_i t}-1)a_i^\dagger]\right)\right|0\right\rangle\ . \qquad (32)$$

The ground-state average is finally obtained by using the relation

$$\langle 0\,|e^{L(a,a^\dagger)}\,|0\rangle=e^{(1/2)\langle 0|L^2|0\rangle}\ ,$$

where $L$ is any linear combination of boson operators $a$, $a^\dagger$. The final result of all this algebra[14] is remarkably simple,

$$P(t)=P_0\exp\left(\sum_i\frac{|I_i|^2}{\hbar^2}e^{-i\omega_i t}\right)\ , \qquad (33)$$

where

$$P_0=\exp\left(-\sum_j\frac{|I_j|^2}{\hbar^2}\right)$$

is a normalization factor such that $\int_{-\infty}^{+\infty}d\omega P(\omega)=1$.

It is easy to establish the connection with the perturbation treatment by expanding (33) in powers of the interaction $|I_i|^2$ and integrating (27):

$$P(\omega)=P_0\sum_{n=0}^{\infty}\frac{1}{n!}\sum_{i_1 i_2\cdots i_n}|I_{i_1}|^2\cdots|I_{i_n}|^2$$

$$\times\delta[\omega-(\omega_{i_1}+\omega_{i_2}+\cdots+\omega_{i_n})]\ . \qquad (34)$$

The term $n=0$ is $P_0\,\delta(\omega)$ and, therefore, $P_0$ gives the strength of the no-loss line. The term $n=1$ gives the classical (Born-approximation) result and describes the loss due to a single-plasmon emission. In the phonon case this first term gives the correct spectrum[4] when $\omega$ is below the threshold $2\omega_T$ for the excitation of two low-frequency surface

TABLE II. Coupling functions $\Gamma_i(k,z_e)$ of the electron with the eigenmodes of the slab, and their Fourier transforms $I_i(\omega)$.

| Eigenmodes | Coupling functions $\Gamma_i$ | | | Integrals $I_i$ |
|---|---|---|---|---|
| | $z_e<-a$ | $-a<z_e<+a$ | $z_e>+a$ | |
| 0+ | $e^{kz_e}$ | $\frac{e^{-ka}}{\cosh ka}\cosh kz_e$ | $e^{-kz_e}$ | $\frac{2k}{k^2+\omega^2/v^2}\ \frac{\cos(\omega a/v)}{v\cosh ka}$ |
| 0− | $-e^{kz_e}$ | $\frac{e^{-ka}}{\sinh ka}\sinh kz_e$ | $+e^{-kz_e}$ | $\frac{2k}{k^2+\omega^2/v^2}\ \frac{i\sin(\omega a/v)}{v\sinh ka}$ |
| $m+$ $(m=1,3,5,\ldots)$ | 0 | $\cos\left(\frac{m\pi}{2a}\right)z_e$ | 0 | $(-1)^{(m-1)/2}\frac{m\pi/a}{\omega_2/v^2-m^2\pi^2/4a^2}\ \frac{\cos(\omega a/v)}{v}$ |
| $m-$ $(m=2,4,6,\ldots)$ | 0 | $\sin\left(\frac{m\pi}{2a}\right)z_e$ | 0 | $-(-1)^{m/2}\frac{im\pi/a}{\omega^2/v^2-m^2\pi^2/4a^2}\ \frac{\sin(\omega a/v)}{v}$ |
| "shear" modes (all $m>0$) | 0 | 0 | 0 | 0 |

phonons. Above $2\omega_T$, many-phonon excitations are found to give small contribution.[4] In the plasmon case, such a threshold does not exist since the lower surface plasmon branch goes to zero in the long-wavelength limit. As a result, any energy $\hbar\omega$ can *a priori* be lost through the excitation of an arbitrarily large number $n$ of these surface plasmons. Such processes are described by the $n$th-order terms in the series (34) which may not converge fast. Therefore, one should first perform the summation over the mode index $i$ in (33) and then introduce the energy conservation through the Fourier transform (27).

### C. Summation over Modes

In the summation of (33)

$$J \equiv A\int d\vec{k}\,J(\vec{k}) = A\int d\vec{k}\sum_{mp}\frac{|I_{mp}(k)|^2}{\hbar^2}\,e^{-i\omega_{mp}(k)t}\,, \tag{35}$$

the $\vec{k}$ integrand $J(\vec{k})$ can be split into two surface terms ($m=0$) and an infinite number of bulk terms ($m\neq 0$). We shall first perform the summation over the bulk modes. Using the definitions (22) and (14) for the $I$ integrals, we have

$$J(\vec{k}) = \textstyle\sum_p Q_p(\vec{k}) + A(\vec{k})\,, \tag{36}$$

where

$$\sum_p Q_p(\vec{k}) \equiv \sum_p \frac{|I_{0p}|^2}{\hbar^2}\,e^{-i\omega_{0p}t} \tag{37}$$

are the two surface terms and

$$A(\vec{k}) = \sum_{m\neq 0,\,p}\int_{-\infty}^{+\infty}\int_{-\infty}^{+\infty} d\tau\,d\tau'\,e^{-i\omega_p(\tau-\tau'+t)}\frac{g_p^2}{\hbar^2}\int_{-a}^{+a}\int_{-a}^{+a} dz\,dz'\,e^{-k(|z-z_e(\tau)|+|z'-z_e(\tau')|)}$$
$$\times e^{-i\vec{k}\cdot[\vec{\rho}_e(\tau)-\vec{\rho}_e(\tau')]}\,\vec{\chi}[z-z_e(\tau)]\cdot\vec{\pi}^*_{mp}(z)\,\vec{\pi}_{mp}(z')\cdot\vec{\chi}[z'-z_e(\tau')] \tag{38}$$

is the bulk contribution. Rewriting the closure relation (7) as

$$\sum_{m\neq 0,\,p}\vec{\pi}^*_{mp}(z)\,\vec{\pi}_{mp}(z') = \overleftrightarrow{E}\,\delta(z-z') - \sum_p \vec{\pi}^*_{0p}(z)\,\vec{\pi}_{0p}(z')\,, \tag{39}$$

we can perform the summation in (38). The result is

$$A(\vec{k}) = B(\vec{k}) - D(\vec{k})\,, \tag{40}$$

where

$$B(\vec{k}) = \frac{g_p^2}{\hbar^2}\,e^{-i\omega_p t}\int_{-a}^{+a} dz$$
$$\times\left|\int_{-\infty}^{+\infty} d\tau\,e^{-i\omega_p\tau-k|z-z_e(\tau)|}\,e^{-i\vec{k}\cdot\vec{\rho}_e(\tau)}\right|^2 \tag{41}$$

is the main bulk contribution arising from the $\delta$ function in (39) and

$$D(\vec{k}) = \sum_p \frac{1}{\hbar^2}\,|I_{0p}(\omega_{0p}\to\omega_p)|^2 e^{-i\omega_p t} \tag{42}$$

is the so-called "begrenzung" term which is obtained from the surface term (37) by replacing the surface mode frequencies $\omega_{0p}$ by the bulk frequency $\omega_p$. The physical meaning of this contribution $D(\vec{k})$ will be discussed later but here let us point out its derivation. It arises from the second term on the right-hand side of the closure relation (39), which can be thought of as a sum rule for all the modes in the slab.

To proceed with the calculation and integrate over the slab and times $\tau$, one has to specify the electron trajectory $[\vec{\rho}_e(\tau), z_e(\tau)]$ in each particular case.

## IV. TRANSMISSION CASE

We shall first apply the results of Sec. III to the case of a transmitted beam at normal incidence. The electron trajectory is then $z_e(t)=vt$, $\vec{\rho}_e(t)=0$. When we insert this into (41) and integrate over momenta we find a periodic bulk contribution to $J$ in (35),

$$B(t) \equiv 2\pi A\int_0^{k_c} k\,dk\,B(k) = \tfrac{1}{2}C\,e^{-i\omega_p t}\ln\left(1+\frac{k_c^2 v^2}{\omega_p^2}\right)\,, \tag{43}$$

where

$$C = 2e^2\omega_p a/\hbar v^2\,, \tag{44}$$

and where $k_c$ is either the wave vector beyond which the continuum approximation would break down or the maximum momentum transfer related to the aperture of the electron spectrometer,[4] whichever of these two limits is lower.

The begrenzung term becomes, after inserting the proper coupling integrals of Table II,

$$D(t) \equiv 2\pi A\int_0^{k_c} k\,dk\,D(k)$$
$$= C\,e^{-i\omega_p t}\,\frac{1}{a}\int_0^{k_c} dk\,\frac{k^2}{(k^2+\omega_p^2/v^2)^2}$$
$$\times\left[\tanh ka\cos^2\left(\frac{\omega_p a}{v}\right)+\coth ka\sin^2\left(\frac{\omega_p a}{v}\right)\right]\,. \tag{45}$$

$D(t)$ oscillates with the same frequency $\omega_p$ as the bulk term $B(t)$, so it will partly compensate the bulk loss. This reduction is a simple geometrical effect

coming from the finite thickness of the slab. It arises from the redistribution of available degrees of freedom when the surface plasmons are included. In the limit of a very thin slab ($a \to 0$), there is exact cancellation of $B(t)$ by $D(t)$, as can be seen from (45).

The surface modes $(\vec{k}, 0, \pm 1)$ give two contributions to $J$,

$$Q_{\pm}(t) \equiv 2\pi A \int_0^{k_c} k\,dk\, Q_{\pm}(k)$$

$$= C\frac{1}{a}\int_0^{k_c} dk\, \frac{k^2}{(k^2+\omega_{\pm}^2/v^2)^2}\,\frac{\omega_p}{\omega_{\pm}(k)}\,(\tanh ka)^{\mp 1}$$

$$\times \begin{pmatrix} \sin^2\left(\frac{\omega_+ a}{v}\right) \\ \cos^2\left(\frac{\omega_- a}{v}\right) \end{pmatrix} e^{-i\omega_{\pm} t}\,, \qquad (46)$$

corresponding to the two branches of the dispersion curve $\omega_{\pm}(k)$. Collecting terms, the correlation function (33) is now given by

$$P(t) = P_0\, e^{J(t)}\,, \qquad (47)$$

where

$$J(t) = A_p\, e^{-i\omega_p t} + Q_+(t) + Q_-(t)\,, \qquad (48)$$

$$A_p = B(0) - D(0)\,. \qquad (49)$$

From (47) and (48) we can now see the general shape of the loss spectrum. The first term in (48), which is periodic in $t$, will give rise to $\delta$ peaks in the loss spectrum at frequencies which are integer multiples of $\omega_p$. The surface terms $Q_{\pm}(t)$ are complicated functions of time containing all frequencies $\omega_{\pm}(k)$, which makes further rigorous analytic treatment very difficult.

In order to extract physical information from (47) and (48) we notice that the flat region $(1/a < k < k_c)$ of $\omega_{\pm}(k)$ will give a nearly periodic contribution to the integrals (46) with the approximate time dependence $e^{-i\omega_I t}$, where $\omega_I = \omega_p/\sqrt{2}$ is the asymptotic surface mode frequency. These contributions will ultimately result in sharp $\delta$-like peaks in the loss spectrum at frequencies which are integer multiples of $\omega_I$. We can separate this part and the one arising from the region of strong dispersion $(0 < k < 1/a)$:

$$Q_+(t) + Q_-(t) \simeq F_+(t) + F_-(t) + A_I\, e^{-i\omega_I t}\,, \qquad (50)$$

where

$$F_{\pm}(t) = C\frac{1}{a}\int_0^{1/a} dk\, \frac{k^2}{(k^2+\omega_{\pm}^2/v^2)^2}\,\frac{\omega_p}{\omega_{\pm}}\,(\tanh ka)^{\mp 1}$$

$$\times \begin{pmatrix} \sin^2\,\dfrac{\omega_+ a}{v} \\ \cos^2\,\dfrac{\omega_- a}{v} \end{pmatrix} e^{-i\omega_{\pm} t}\,, \qquad (51)$$

$$A_I \simeq C\frac{1}{a}\int_{1/a}^{k_c} \frac{\sqrt{2}\,k^2\,dk}{(k^2+\omega_I^2/v^2)^2}\,. \qquad (52)$$

In deriving (52) we have used the approximations

$$\left.\begin{aligned} &\omega_{\pm}(k) \simeq \omega_I \\ &\tanh ka \simeq \coth ka \simeq 1 \end{aligned}\right\} \text{ for } k > 1/a\,. \qquad (53)$$

From (51) and (52) we can see the dependence of (50) on the slab thickness. For large $a(k_c a \gg 1)$, the interval $1/a < k < k_c$ covers essentially all available $k$ space so that the $A_I$ contribution and, therefore, the $\delta$-like peak at $\omega_I$, dominate. For a thin slab $(1/a \to k_c)$, $A_I$ goes to zero, the peak disappears and the broad structure given by $F_{\pm}$ dominates. In this case, the bulk peak at $\omega = \omega_p$ is also suppressed due to the begrenzung effect, $A_p \to 0$.

It is necessary to notice that the peaks at $\omega$ equal to an integer multiple of $\omega_I$ are not exactly $\delta$ functions although they are very sharp for large thickness. One can also show that single-plasmon contributions are zero at $\omega = \omega_I$. However, this narrow dip in the spectrum could be filled as a result of many-plasmon processes and we shall return to this point later.

We may now write the loss function in the form

$$P(\omega) = \frac{1}{2\pi}\,P_0 \int_{-\infty}^{+\infty} e^{i\omega t}$$

$$\times \exp\left(A_p e^{-i\omega_p t} + A_I e^{-i\omega_I t}\right)\, e^{F(t)}\,dt\,, \qquad (54)$$

where

$$F(t) = F_+(t) + F_-(t) \qquad (55)$$

is an aperiodic function which vanishes for large $t$ (compared to $1/\omega_p$). By writing $e^F = 1 + (e^F - 1)$ in (54) we can separate the periodic part responsible for electron losses at discrete energies from the aperiodic part which gives rise to the continuous broad structure. Expanding the periodic part, which is allowed for discrete energy transitions, one finally obtains

$$P(\omega) = \Delta(\omega) + S(\omega)\,, \qquad (56)$$

$$\Delta(\omega) = P_0 \sum_{m,n=0}^{\infty} J_{mn}\,\delta[\omega - (m\omega_p + n\omega_I)]\,, \qquad (57)$$

$$S(\omega) = P_0 \sum_{mn} J_{mn} S^0[\omega - (m\omega_p + n\omega_I)]\,, \qquad (58)$$

where

$$J_{mn} = \frac{A_p^m A_I^n}{m!\,n!}\,, \qquad (59)$$

$$S^0(\Omega) = \frac{1}{2\pi}\int_{-\infty}^{+\infty} e^{i\Omega t}\,(e^{F(t)} - 1)\,dt\,. \qquad (60)$$

$\Delta(\omega)$ represents the series of discrete $\delta$ peaks with strengths given by $J_{mn}$. For $A_p$ or $A_I > 1$ the

maximum strength will occur at $m$ or $n > 1$, i.e., for the emission of several plasmons. The strengths and envelopes of these peaks are given in Fig. 3 for various $A_p$ or $A_I$.

$S(\omega)$ describes the series of broader structures, all with the same shape given by $S^0(\Omega)$, positioned at $m\omega_p + n\omega_I$ and with relative strengths $J_{mn}$. In practice there will be only one such contribution of appreciable strength (for $m = n = 0$) because $S^0(\Omega)$ becomes significant only for thin films, in which case $A_p$ and $A_I$ go to zero.

The importance of many-plasmon effects for the shape of $S^0(\Omega)$ is determined by the value of $F(t)$. If $F(t)$ is small, the spectrum will be given mainly by one-plasmon contributions and the classical (or first-order perturbation) result will be valid. When $F(t)$ is large, many-plasmon emission will drastically change the shape of $S^0(\Omega)$. The order of magnitude of, say, $F_-(t)$ can be found from

$$F_-(0) \simeq C\frac{1}{a}\int_0^{1/a} \frac{k^2\,dk}{(k^2+\omega_-^2/v^2)^2}\,\frac{\omega_p}{\omega_-}\tanh ka\ , \qquad (61)$$

$$F_-(0) \simeq \frac{2e^2}{\hbar v}\left[\tan^{-1}\left(\frac{v}{\omega_p a}\right) - \frac{\omega_p a/v}{1+\omega_p a^2/v^2}\right]\ , \qquad (62)$$

where we have used the approximation $\omega_-(k) \simeq \omega_p \times (ka)^{1/2}$. This gives

$$F_-(0) \simeq \begin{cases} \frac{2}{3}\,\frac{2e^2}{\hbar v}\left(\frac{v}{\omega_p a}\right)^3 & \text{for } \frac{\omega_p a}{v} \gg 1 \qquad (63) \\ \frac{1}{2}\,\frac{2e^2}{\hbar v}\,\pi & \text{for } \frac{\omega_p a}{v} \ll 1\,. \qquad (64) \end{cases}$$

For silver ($\hbar\omega_p \sim 4$ eV), with $a = 200$ Å and $v \simeq 10^{10}$ cm/sec (25-keV electrons), one finds $\omega_p a/v \simeq 2$ and $2e^2/\hbar v \simeq 0.05$. This means that in the usual loss experiment on metallic films at normal beam incidence, the integral in (61) does not provide the increase in $F$ necessary to boost the many-plasmon emission. The main reason for it is the shape of the dispersion curve $\omega_-(k)$ for $k \to 0$: Because of the infinite slope at the origin, the phase space for low-energy plasmon excitations is too small. However, many-plasmon effects can become appreciable if we lower the electron velocity or reduce the angle between the beam and the surface, as will be discussed later.

In very thin semiconductor films for which plasmon energies are small, one could observe the characteristic shape of the loss spectrum due to multiple-plasmon emission. Figure 4 shows the function $S^0(\omega)$ numerically calculated for such a case, with parameters $a = 50$ Å, $\omega_p = 10^{15}$ sec$^{-1}$, and $v = 0.3\times10^9$ cm/sec. One can see a strong characteristic many-plasmon tail for $\omega > \omega_p$ extending towards high energies where single-plasmon processes cannot contribute. This tail, together with the enhancement of the main part in the interval $0 < \omega < \omega_p$, is due to the possibility of recombination of many emitted surface plasmons for any given energy loss. The dips at $\omega_I$ and $\omega_p$ are partially filled, as mentioned earlier, though the peaks on both sides of each dip are still visible. Small wiggles in the curve are probably spurious and due to computing inaccuracy.

Similar spectra could also be expected for heavier charged particles, e.g., protons or ions, transmitted through metallic or semiconductor films, if other types of scattering can be discriminated.

## V. REFLECTION CASE

### A. Formulas for General Incidence

We shall now apply the formalism of Sec. III to the case where the electrons strike the surface at some angle $\theta$ and are specularly reflected, as shown in Fig. 5. Let us assume that the electrons do not penetrate into the slab more than a few atomic

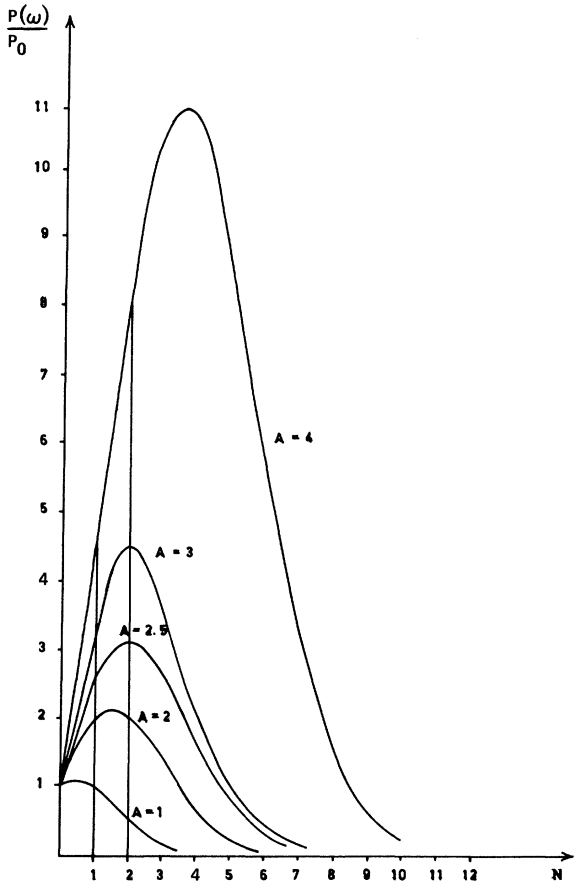


FIG. 3. Strengths and envelopes of the multiple-plasmon loss peaks relative to the no-loss line as functions of the number $N$ of emitted plasmons (either volume plasmons at $\omega_p$ or surface plasmons at $\omega_I = \omega_p/\sqrt{2}$). The parameter $A$ is the coupling strength $A_p$ or $A_s$, Eqs. (49) and (52).

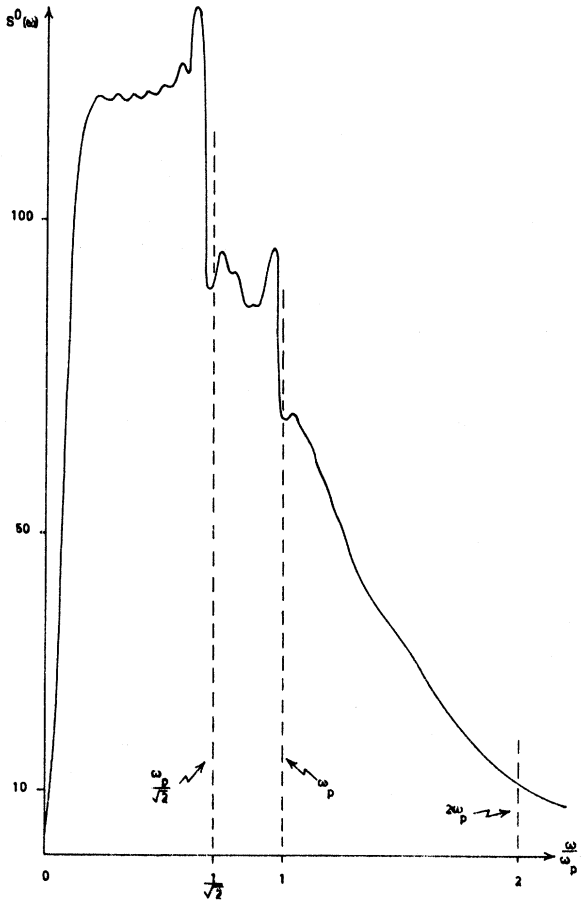


FIG. 4. Computed loss spectrum $S^0(\omega)$ defined in Eq. (60). The tail for $\omega > \omega_p$ comes from the multiple surface-plasmon emission.

layers. This assumption is valid when the normal electron velocity $v_\perp$ is small. Then the reflected electrons couple only to the surface modes and the trajectory is given by

$$\vec{r}_e(t) = [\vec{\rho}_e(t),\ z_e(t)],$$
$$\vec{\rho}_e(t) = -\vec{v}_\parallel t, \quad z_e(t) = -v_\perp |t| - a. \tag{65}$$

The coupling functions $\Gamma_\pm(\vec{r}_e)$ corresponding to the two surface plasmon modes are (from Table II)

$$\Gamma_\pm(\vec{r}_e) = \mp g_\pm \left(\frac{\sinh 2ka}{k}\right)^{1/2} e^{kz_e}. \tag{66}$$

The $I$ integrals (22) appropriate to the trajectory (65) are found to be

$$I_\pm(k) = \mp g_\pm \left(\frac{\sinh 2ka}{k}\right)^{1/2} e^{-ka} \frac{2kv_\perp}{(\omega_\pm - \vec{k}\cdot\vec{v}_\parallel)^2 + k^2 v_\perp^2}. \tag{67}$$

Let us consider a very thick slab ($a \to \infty$) where the two surface modes are degenerate at $\omega_\pm(k) = \omega_I$. Introducing (67) into (33), where the summation over the modes reduces to a $\vec{k}$ integration, one obtains

$$P(\omega) = \frac{1}{2\pi} P_0 \int_{-\infty}^{+\infty} dt\, e^{i\omega t} \exp(Q\, e^{i\omega_I t}), \tag{68}$$

$$Q = \frac{\sqrt{2}\, e^2 \omega_p}{\pi\hbar} \int_0^{k_c} dk \int_0^{\pi} d\varphi \frac{k^2 v_\perp^2}{[(\omega_I - kv_\parallel \cos\varphi)^2 + k^2 v_\perp^2]^2}, \tag{69}$$

where $\varphi$ is the angle between $\vec{k}$ and $\vec{v}_\parallel$. This double integration can be done exactly,[15] but let us consider the simple cases of normal and grazing angle incidence.

### B. Normal Incidence

For normal or nearly normal incidence, which is the case in most LEED measurements, we have $v_\perp \gg v_\parallel$ and (69) can be easily evaluated to give

$$Q = \frac{e^2 \omega_p}{\sqrt{2}\hbar v_\perp^2} \left[\frac{v_\perp}{\omega_I} \tan^{-1}\left(\frac{k_c v_\perp}{\omega_I}\right) - \frac{k_c}{k_c^2 + \omega_I^2/v_\perp^2}\right]. \tag{70}$$

As an example, we take the electron beam of velocity $v_\perp = 0.5 \times 10^9$ cm/sec (energy $\simeq 80$ eV) reflected from the surface of silver. One finds $Q \simeq 1$. Expanding (68) in powers of $Q$ one sees that the loss contains not only the lowest-order contribution due to single-plasmon emission, but also a number of strong peaks corresponding to multiple-plasmon emission. The curve for $A = 1$ on Fig. 3 gives the strengths of these peaks for several orders of plasmon excitation.

In the LEED case considered here, the electron energies are too low to justify the approximation of neglecting the electron recoil. The decrease of velocity causes two mutually competing and opposite effects: (a) The electron spends more time in the vicinity of the surface, which increases the emission of surface plasmons. (b) The effect of the recoil dampens the scattering and ultimately destroys the correlation between successive processes and thus washes away the many-plasmon contribution.

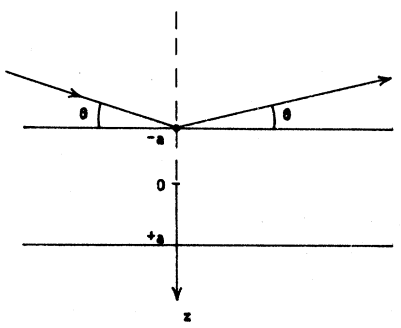


FIG. 5. Geometry of the reflection experiment using beams at oblique incidence.

However, this result, together with those obtained for very thin films, is a clear indication that at low or intermediate energies it would be necessary to consider (in some improved model) many-plasmon emission when analyzing inelastic processes.

### C. Grazing-Angle Incidence

Much more obvious is the contribution of many-plasmon processes in the scattering of high-energy electrons from the surface at grazing incidence. Here we increase the scattering while still keeping the recoil negligible. Because of the condition $v_\perp \ll v_\parallel$ we can use the approximation

$$\lim_{v_\perp/v_\parallel \to 0} \frac{kv_\perp}{(\omega_I - kv_\parallel \cos\varphi)^2 + k^2 v_\perp^2} = \pi\delta(\omega_I - kv_\parallel \cos\varphi), \tag{71}$$

which enables us to perform the $\varphi$ integral in (69) in a trivial manner

$$Q = (2e^2/\hbar v_\perp)\,\alpha I(\alpha), \tag{72}$$

where

$$\alpha = \omega_p/\sqrt{2}\,k_c v_\parallel, \tag{73}$$

$$I(\alpha) = \int_\alpha^1 d\mu\, \frac{(\mu^2 - \alpha^2)^{1/2}}{\mu^3}. \tag{74}$$

This last integral can be done exactly, but in view of the approximation (71) we need only to use the limit

$$\lim_{\alpha \to 0} \alpha I(\alpha) = \tfrac{1}{4}\pi + 0(\alpha). \tag{75}$$

The physical meaning of the approximation (71) is that the electron which spends a sufficiently long time near the surface interacts resonantly with those surface plasmons which have phase velocity $\omega_I/(k\cos\varphi)$ equal to the parallel velocity $v_\parallel$.

If we now reconsider our previous example of a thick silver slab but using 10-keV electron beam at $\theta = 1.5°$ incidence, we get $v_\parallel \simeq 0.6\times10^{10}$ cm/sec and a very low $v_\perp \simeq 2.10^8$ cm/sec. From (73) follows $\alpha = 0.1$, which confirms our limit (75), and from (72) one finds $Q = 2.5$. When this $Q$ is inserted into (68) we get a series of $\delta$ peaks in the loss spectrum positioned at multiples of $\omega_I$ and with strengths given in Fig. 3.

The classical theory could only predict the one-plasmon loss peak at $\omega = \omega_I$. Instead, we find that the spectrum will be dominated by the multiple excitations and this cannot be explained within the first Born approximation for the transitions between the quantized states of the plasmon field. Such multiple emissions of surface plasmons have been observed by Powell,[16] and both the separation and strength of the successive peaks are in agreement with the predictions of the present theory.

### D. Very Thin Film at Grazing Incidence

The dependence of the loss spectrum on the slab thickness at the grazing-angle condition can be determined by using the nondegenerate dispersion relation $\omega_\pm(k)$ in the expression (67) for $I_\pm(\vec{k})$ and integrating to obtain $Q_\pm(t)$, which would contain all surface-plasmon frequencies.

Let us here consider the limit of a very thin film ($k_c a \ll 1$), where the peak at $\omega = \omega_I$ disappears. In this case the reflection and transmission experiments should give basically similar results because the bulk contribution at $\omega = \omega_p$ is also completely cancelled by the begrenzung term. In the resulting electron-loss spectrum we expect to observe only the many-plasmon contribution from the strongly aperiodic part of $\omega_\pm(k)$, with the same shape that was already shown in Fig. 4 for the case of a transmitted beam.

## VI. CONCLUSION

In this paper we have developed a quantum-mechanical theory of the fast-electron-plasmon interaction in a slab, including explicitly the surface effects. Retardation effects and excitation damping have been neglected. The main results can be summarized as follows:

(a) We have obtained a complete description of the fast-electron-loss spectrum as a function of several parameters $(a, \omega_p, v, \theta)$. In particular, the origin of the begrenzung effect has been elucidated and the thickness dependence of various contributions calculated.

(b) Multiple-plasmon emission, which cannot be described by classical theory, has been shown to influence both the sharp peaks in the spectrum associated with discrete energy losses and the broad structures due to the emission of strongly dispersed surface plasmons. These many-body effects turn out to be important for the large "fine-structure constant" $e^2/\hbar v_\perp \gtrsim 1$, a condition which is realized either in LEED or in the usual high-energy electron beams at grazing incidence.

Because of its generality and rather simple form, this theory could be easily extended to a number of connected problems. Its application to the electron-phonon coupling at polar crystal surfaces can immediately explain the observed shape and magnitude of many-phonon contributions in the loss spectra of both specularly and Bragg-reflected beams.[17] For thin films where the explanation given in Ref. 17 cannot be applied, our theory predicts additional structures originating from the strong dispersion of the surface modes.

When thin metallic films are deposited on a dielectric substrate with dielectric constant $\epsilon > 1$, a gap exists in the surface plasmon energies [see Fig. 1(b)] and in the single-plasmon excitation spectrum and, hence, this gap should be reproduced in the electron-loss spectrum if only single-plasmon processes contributed. Many-plasmon excitations,

when present, can occur in this gap and partly fill it so that such experiments could provide another check of the present theory.

Another case where fast-electron energy losses were observed is x-ray photoemission,[18] where the electron created in the solid can excite both bulk and surface plasmons. The extension of our theory to this case could be worked out,[15] though the situation here is more complicated by the presence of the hole. Its lifetime and the relaxation of the Fermi sea via low-energy electron-hole pair excitations modify the shape of the emitted-electron spectral lines.[19] These effects could be treated independently of the discrete plasmon losses, but in thin films they might interfere with the surface plasmon emission from the region of strong dispersion.

ACKNOWLEDGMENTS

The authors would like to thank Professor Abdus Salam, the International Atomic Energy Agency, and UNESCO for hospitality at the International Centre for Theoretical Physics, Trieste. They are also grateful to Professor S. Lundqvist for critical reading of the manuscript and Dr. R. Guardiola for help with numerical analysis.

*Permanent address: Institute Rudjer Bošković, Zagreb, Yogoslavia.

†Chargé de Recherches au Fonds National Belge de la Recherche Scientifique. Present address: European Space Research Organization, Noordwyk, Holland.

[1]See, e.g., D. Pines, *Elementary Excitations in Solids* (Benjamin, New York, 1964).

[2]For further references see, H. Raether, *Springer Tracts in Modern Physics* (Springer, Berlin, 1965), Vol. 38, p. 84.

[3]J. Geiger and K. Wittmaack, Z. Physik 195, 44 (1966).

[4]A. A. Lucas, E. Kartheuser, and R. Badro, Solid State Commun. 8, 1075 (1970); Phys. Rev. (to be published).

[5]In the LEED case, however, the recoil of the electron in the plasmon emission cannot be neglected.

[6]J. B. Chase and K. L. Kliewer, Phys. Rev. (to be published). We thank the authors for sending us the preprint of this work prior to publication.

[7]M. Šunjić, A. A. Lucas, and M. Tomaš (unpublished).

[8]The application of the theory to the electron-phonon coupling is straightforward.

[9]R. Fuchs and K. L. Kliewer, Phys. Rev. 140, 2076 (1965).

[10]M. Born and K. Huang, *Dynamical Theory of Crystal Lattices* (Clarendon, Oxford, England, 1966).

[11]The $S$ polarization eigenmodes do not couple to the electron.

[12]The present derivation of the dielectric properties of the free-electron gas from those of an ionic plasma is similar to a recent study where the Wigner electron lattice is described as a limiting case of the classical Lorentz lattice, see A. Bagchi, Phys. Rev. 178, 707 (1969).

[13]E. N. Economou, Phys. Rev. 182, 539 (1969).

[14]A treatment formally similar to ours has been recently applied, e.g., in the x-ray problem, by K. D. Schotte and U. Schotte, Phys. Rev. 182, 479 (1969), to the singular electron-hole pair scattering, and by D. C. Langreth, Phys. Rev. B 1, 471 (1970) to the deep hole screening by plasmons in the uniform electron gas.

[15]M. Šunjić and A. A. Lucas (unpublished).

[16]C. J. Powell, Phys. Rev. 175, 972 (1968).

[17]H. Ibach, Phys. Rev. Letters 24, 1416 (1970).

[18]See, e.g., S. Hagström, C. Nordling, and K. Siegbahn, in *Alpha-, Beta- and Gamma-Ray Spectroscopy*, edited by K. Siegbahn (North-Holland, Amsterdam, 1965), p. 845.

[19]S. Doniach and M. Šunjić, J. Phys. C 3, 285 (1970).

PHYSICAL REVIEW B VOLUME 3, NUMBER 3 1 FEBRUARY 1971

# Analysis of the Magnetic Susceptibility of $K_2OsCl_6$

H. U. Rahman

*Department of Mathematics, Heriot-Watt University, Edinburgh, United Kingdom*

(Received 1 July 1970)

The configuration interaction between the $t_2^4$ and $t_2^3e$ configurations has been taken into account to calculate the energy levels of the $(OsCl_6)^{2-}$ complex ion in the intermediate-coupling scheme. The matrix elements of the magnetic moment operator between the ground level $A_1$ and the excited $T_1$ levels are given in algebraic form, and then used to calculate the temperature-independent paramagnetic susceptibility. The experimental value of the susceptibility and a part of the optical absorption spectrum can be fitted to theory by choosing the following values of the parameters: $B = 365.5$ cm$^{-1}$, $C = 1561.0$ cm$^{-1}$, $\zeta_{5d} = 2575.0$ cm$^{-1}$, $\Delta = 33\,000.0$ cm$^{-1}$, $k = 0.7$, $k' = 0.7$.

## I. INTRODUCTION

In complexes of the type $X_2YZ_6$, where $X$ is an alkali ion [(or $NH_4$, $C(NH_3)_4$, etc.)], $Y$ is a metal ion of the $4d$ or $5d$ group, and $Z$ is a halogen ion, unlike the corresponding complexes of the iron